PICO-SCALE OPEN FLUME PROPELLER WATER TURBINE PERFORMANCE UNDER VARIATION IN AIRFOIL THICKNESS-TO-CHORD RATIO

CHRISTIAN ROMULUS TIGOR[1], WARJITO[1*], BUDIARSO[1], AJI PUTRO PRAKOSO[2]

[1]*Mechanical Enigneering Department, Faculty of Engineering, Universitas Indonesia, Depok 16424, Indonesia*
[2]*Mechanical Engineering Program, Faculty of Engineering, Universitas Pembangunan Nasional 'Veteran' Jakarta, Depok 16514, Indonesia*

**Corresponding author: warjito@eng.ui.ac.id*

(Received: 4 May 2026; Accepted: 11 June 2026; Published online: 01 July 2026)

ABSTRACT: Air pollution from coal-fired power plants contributes approximately 44% of Indonesia's CO_2 emissions. Transitioning to renewable sources, such as hydroelectric power, offers a viable solution, particularly with open-flume propeller turbines in remote areas. This study investigates the effect of T/C ratios on pico-scale open-flume propeller turbines using NACA 44XX airfoils. Three configurations (0.11, 0.12, and 0.13) with varying rotational speeds were evaluated using computational fluid dynamics (CFD) simulations with mesh motion in ANSYS Fluent, along with analytical methods for torque, power output, and efficiency. T/C 0.13 consistently delivered the best performance, reaching a maximum efficiency of 15.39% at 850 rpm. In contrast, the analytical method found that the maximum efficiency of that configuration is approximately 26% at 1100 RPM. The deviation between the analytical and numerical results arises from the analytical method's limitations in capturing the viscous shear flow around the turbine blades and the gap-clearance loss. The pressure distribution analysis revealed that T/C 0.13 maintained the most balanced high–low pressure zones, minimizing early flow separation. T/C 0.12 exhibited instability at high RPM due to less stable pressure differentials, whereas T/C 0.11 maintained stability with sharper pressure gradients and a higher risk of separation despite lower output. These findings emphasize the role of optimal blade geometry in improving efficiency, pressure–velocity stability, and flow control in small-scale water turbines. However, the lack of experimental testing in this study limits the validity of its results; further experimentation is needed.

KEY WORDS: Thickness; Chord, Propeller; Open flume; Pico hydro.

1. INTRODUCTION

Indonesia is currently facing a serious air pollution crisis caused by emissions from transportation, industrial activities, and coal-fired power plants (CFPPs), particularly in major urban areas such as Jakarta [1]. This pollution has a severe impact on public health and is a significant contributor to reduced life expectancy [2]. According to data from the IEA [3], CFPPs account for over 50% of the country's total CO_2 emissions, posing a major challenge in air pollution control [4].

The government is promoting an energy transition toward renewable energy sources, such as solar, wind, and hydropower, to address this issue. However, the use of renewable energy potential remains significantly low compared with the available capacity [5]. One efficient and environmentally friendly solution is to implement small-scale hydropower plants, particularly in remote areas.

PHPs are small-scale hydropower systems (ranging from 1000 W to 5 kW) that operate under low-head conditions and are environmentally friendly [6]. Their advantages include simple design, low operating costs, and the ability to integrate with irrigation networks, making them well-suited for rural and remote regions [7]. Turbine selection in PHP depends on the flow type and available head, with two main classifications: impulse turbines (such as Pelton and Turgo) for high-head, low-flow conditions, and reaction turbines (such as Kaplan and Francis) for low- to medium-head with higher discharge [8]. Figure 1 illustrates that Kaplan turbines are particularly suitable for ultra-low-head conditions (down to 1 m) with flow rates between 0.4–0.9 m³/s, making them highly relevant for power generation systems in regions with low-head river flows.

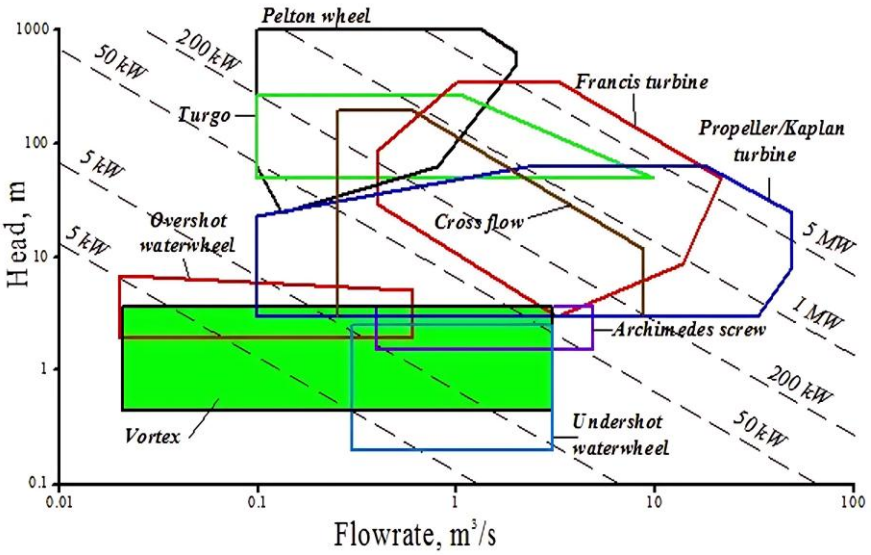

Fig. 1. Application range of water turbines [9]

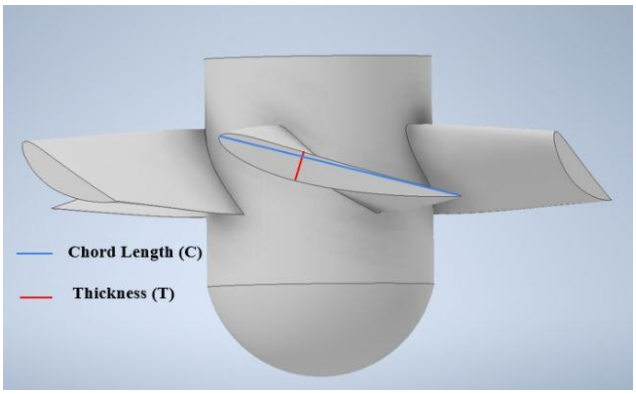

Fig. 2. Thickness and Chord of an Airfoil

Figure 2 shows the turbine blade profile, emphasizing the chord length (C) in blue and the maximum thickness (T) in red. The thickness-to-chord ratio (T/C) is a critical design parameter that significantly influences the aerodynamic performance of the blade, particularly lift generation and flow stability [10]. Previous studies on the blade thickness of propellers or Kaplan turbines usually focus on design and construction strength criteria [11], [12]. Despite the well-known importance of T / C in hydrodynamics, its effect on pico-scale OFP turbines remains underexplored. Among other studies on the thickness of propeller and Kaplan turbine blades [11], [12], [13], this study focuses on the impact of blade thickness on the hydrodynamic

performance of pico-scale propeller OFTs. This study aims to evaluate the effects of T/C ratios (0.11, 0.12, and 0.13) on the torque, power output, and efficiency of a pico-scale OFT.

2. MATERIALS AND METHODS

2.1. Materials

In this study, the turbine blade design process adopted an airfoil profile approach based on the National Advisory Committee for Aeronautics (NACa) standard. NACA is a U.S. federal agency that makes various airfoil geometries for aerodynamic applications, including the widely used 4-digit series in fluid engineering design.

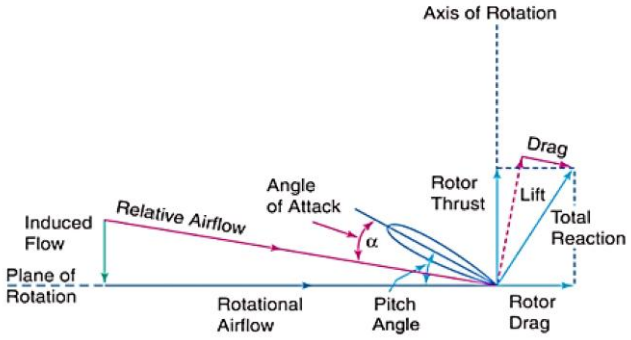

Fig. 3. Forces acting on the airfoil [14]

Thus, the NACA 44xx series profile possesses a distinctive combination of camber and thickness, making it well-suited for applications requiring high lift generation while maintaining flow stability—particularly in low-speed, small-scale water turbine designs such as open flume systems [14]. One of the key parameters is the thickness-to-chord ratio (T/C), which significantly influences the distribution of the lift coefficient (C_L) and drag coefficient (C_D) on the blade surface.

$$F_L = 1/2 \times \rho \times v^2 \times A_{foil} \times C_L \quad (1)$$

$$F_D = 1/2 \times \rho \times v^2 \times A_{foil} \times C_D \quad (2)$$

$$C_N = \frac{2\pi \sin(\theta)}{4+\pi \sin(\theta)} \times \frac{1.98}{0.88} \quad (3)$$

$$C_L = C_N \times \cos(\theta) \quad (4)$$

$$C_D = C_N \times \sin(\theta) \quad (5)$$

Shaft power is the mechanical power generated by the turbine and transmitted to the shaft. This power results from the conversion of a portion or all of the available hydraulic power through the turbine blades [15].

$$P_{shaft} = T \times \omega \quad (6)$$

The torque can be calculated using the following equation:

$$T = \sum(F_L \cos(\beta_1) + F_D \sin(\beta_1)) \times r \quad (7)$$

The hydraulic power is the fluid energy available to the turbine for conversion into mechanical energy [16], [17]. The general formula is:

$$P_h = \eta_h \rho g Q H \quad (8)$$

The turbine efficiency is defined as the ratio between the power output generated by the turbine and the available power within the fluid, which can be calculated using the following equation:

$$\eta = \frac{P_{shaft}}{P_h} \times 100\% \quad (9)$$

2.2. Methods

2.2.1. Analytical Method

This study primarily focused on the design of rotor blades. The hub-tip diameter, number of blades, blade angles, and blade profile are key components in rotor blade design. All other study parameters were kept constant. The hub-tip diameter calculation was based on previous research that employed the same flow rate (Q) and head (H), 41 l/s and 2.71 m, respectively. The selected tip diameter (D_{tip})) was 0.125 m, the hub diameter (D_{hub}) was 0.05 m, and the rotational speed (N) was 1500 rpm.

Table 1: Summary of the design variables

Turbine Type	Propeller
Blade Shape	NACA Seri-4
Number of blades	5
Diameter Tip	0,125 m
Diameter Hub	0,05 m
Hub-to-tip ratio	0,4
Head	2,71 m
Flowrate	40 l / s
Chord length at the hub	0,0283 m
Chord length at tip	0,055 m
Guide vane height	0,05 m
Radius of the Guide Vanes	0,03125
Inlet diameter of the draft tube	0,1377 m
Outlet Diameter of the Draft Tube	0,2678 m
Draft tube height	0,4131 m

2.2.2. Numerical Method

Upon completion of the CAD geometry, transient simulations were conducted in ANSYS Fluent using a two-zone fluid domain connected through an interface: a stationary region and a rotating inner domain. The SST k–ω turbulence model was applied with liquid water as the working fluid, and second-order discretization schemes were implemented. The mesh motion was activated in the rotating domain with rotational speeds ranging from 850 to 1500 rpm. Boundary conditions included a velocity inlet, a pressure outlet, and no-slip walls, using the coupled solver scheme.

To ensure that the simulation results were not significantly influenced by mesh resolution, a mesh-independence study was conducted using the GCI approach. This method evaluates the sensitivity of the results to grid size and guarantees spatial convergence. The primary parameter assessed was the turbine blade torque, which directly correlates with the power output [18]. Three mesh configurations with different element counts were tested sequentially, from the finest to the coarsest.

Table 2: Grid independence study in the simulation of open-flume turbines

Normalized grid spacing	Mesh Elements	Torque	r	p	GCI%
1.31	2248269	1.26 N·m	-	-	-
1.19	2952889	1.18 N·m	1.1	-	2.575%
1.00	5004034	0.9 N·m	1.19	16.0277	2.47%

The thickness-to-chord (T/C) ratio is a critical design variable that influences the hydrodynamic performance of turbine blades. In this study, the T/C ratio was varied by adjusting the airfoil thickness while keeping the chord length constant. This modification enables the evaluation of its impact on torque and overall efficiency. Three blade configurations were tested with T/C values of 0.11, 0.12, and 0.13 (Fig. 5), enabling a systematic analysis of the geometric influence on flow behavior and energy conversion.

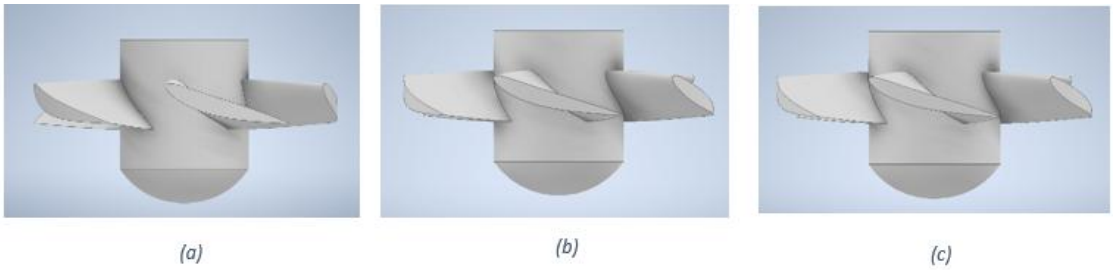

Fig. 5. Blades of turbine at different T/C: (a) T/C 0.11, (b) T / C 0.12, and (c) T/C 0.13

3. RESULT

Figure 6 illustrates the relationship between turbine efficiency (%) and rotational speed (RPM) for three thickness-to-chord (T/C) ratios (0.11, 0.12, and 0.13), comparing numerical and analytical results. In general, all configurations exhibit a decreasing efficiency trend as RPM increases from 850 to 1500, indicating reduced effectiveness of fluid-to-mechanical energy conversion at higher rotational speeds due to increased hydrodynamic losses and reduced flow stability.

The T/C 0.13 configuration consistently records the highest efficiency across the entire RPM range. For instance, at 850 RPM, the analytical result reached approximately 26%, outperforming other configurations and maintaining its superiority up to 1500 RPM with approximately 13% efficiency. Numerical results at the same speed also show T/C 0.13 leading, although at a lower percentage (~15%), still above other ratios.

All three configurations reach their peak efficiency within the low-rotational-speed range of 850–1100 rpm. At 850 RPM, the numerical results for all configurations are nearly equivalent, around 15%, indicating effective energy conversion at low speeds. At 1100 RPM, T/C 0.13 still holds the advantage, achieving 14.25% efficiency, reflecting its ability to maintain stable flow and lift generation. As the speed increases to 1350–1500 RPM, the efficiency drops for all cases, with T/C 0.12 showing the steepest numerical decline to just 6.46%, while the analytical trends also display a similar but less pronounced drop.

The close agreement between analytical and numerical patterns validates the observed performance trends, confirming that a higher T/C ratio (0.13) yields better efficiency retention across varying rotational speeds.

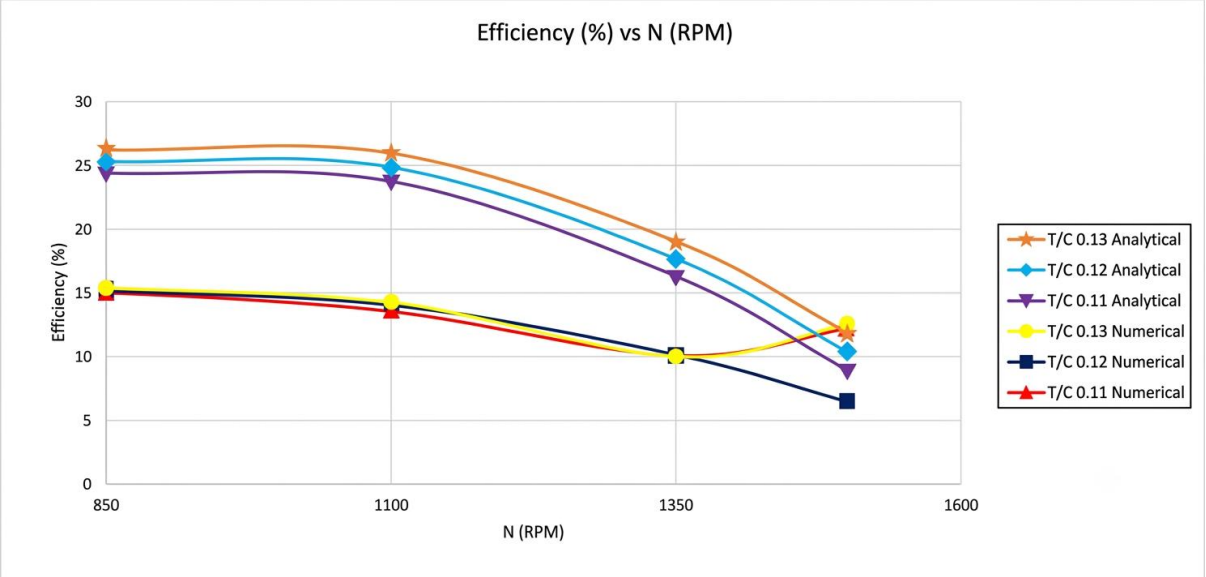

Fig. 6. Efficiency versus RPM (analytical and numerical)

4. DISCUSSION

The instability observed in the T/C = 0.12 numerical configuration can be explained by analyzing the pressure difference (ΔP) between the upper (suction) and lower (pressure) surfaces of the blade section, as shown in Figure 7. In turbine hydrodynamics, the lift force (F_L) generated by an airfoil is directly proportional to this pressure difference, as expressed by Bernoulli's principle and the lift equation:

$$\Delta P = P_{pressure} - P_{suction} \quad (10)$$

$$F_L = \Delta P \times A_{foil} \quad (11)$$

$$F_L = 1/2 \times \rho \times v^2 \times C_L \times A_{foil} \quad (12)$$

For T / C = 0.12, the simulation results indicate that ΔP is smaller and less stable compared to T / C = 0.11 and T / C = 0.13. The reduced high-pressure region on the lower surface and the narrower low-pressure zone on the upper surface lead to a weaker, fluctuating cap F sub cap L. This phenomenon can be attributed to an unfavorable balance between thickness and chord length: the blade profile is insufficiently thick to maintain a strong pressure gradient (as in T/C = 0.13), yet thick enough to disturb laminar flow stability at higher RPM (compared to T/C = 0.11).

At a high rotational speed of 1500 RPM (Figure 7), the unsteady ΔP promotes early flow separation on the suction side. This reduces the effective C_L and increases C_D (drag coefficient), lowering the lift-to-drag ratio (L/D) and, consequently, the turbine's efficiency:

$$\eta \propto C_L/C_D \quad (13)$$

A drop in C_L or a rise in C_D at constant RPM directly translates into a reduction in shaft torque and power output, explaining the steep decline in numerical efficiency to 6.46% for T/C = 0.12. These findings are consistent with those of Kaya et al. (2021) [19], who reported that a higher and more stable pressure difference across an airfoil surface is essential for maintaining lift and delaying separation, while intermediate thickness ratios may fall into a performance "gap" where neither lift stability nor drag minimization is optimized.

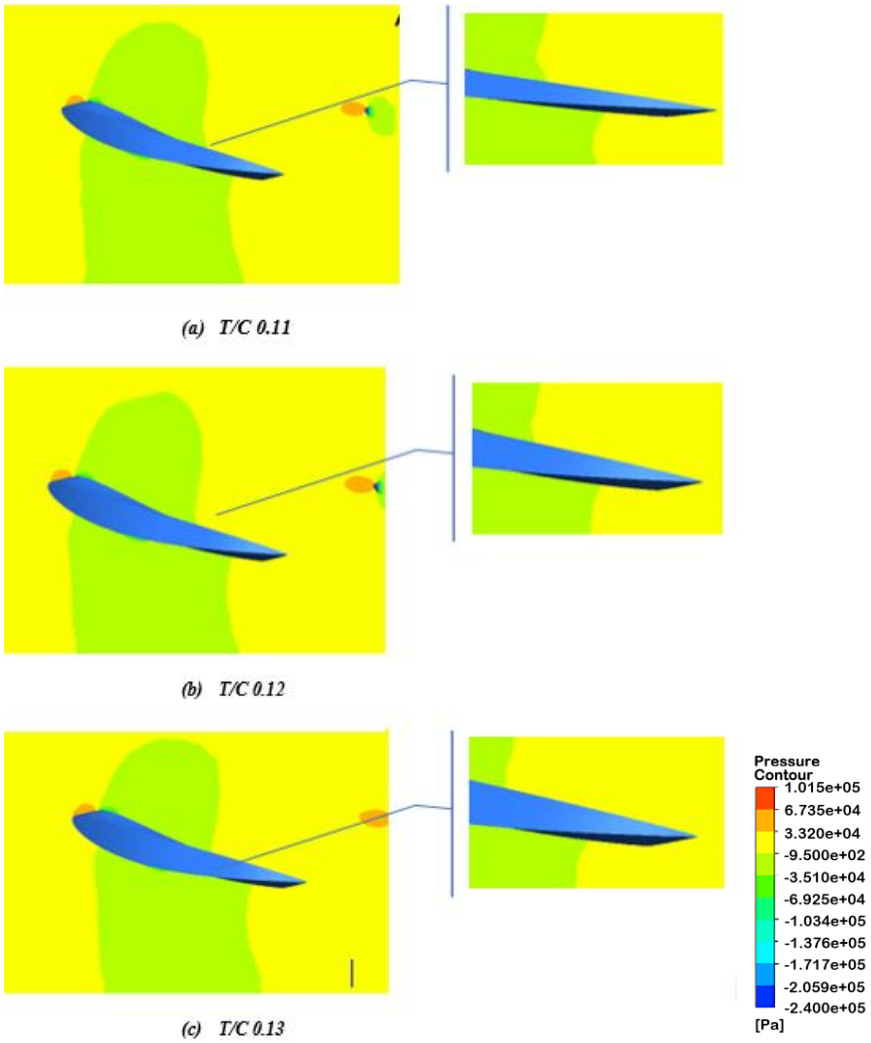

Fig. 7. Pressure Contour at the Mid-Span of the Blade at 1500 RPM

The deviation between the analytical estimation and the numerical approach is mainly due to the limitations of the estimation. The first limitation is that the Euler-Bernoulli-based blade element and momentum theory neglects the blades' viscous effects. In addition, this theory neglects the effects of Reynolds number variation, twist, and radial velocity, and it calculates blade performance at a single radial location. The second limitation is that the analytical estimation cannot calculate the volumetric loss of water flow at the gap between the runner and the pipe and at the gap between the blades. Moreover, the shear stress produced by the swirling flow before the water reaches the turbine cannot be determined analytically. These limitations generate around 8% of the efficiency deviation in this study.

5. CONCLUSION

The results show that the T/C 0.13 configuration achieves the highest efficiency across all tested speeds, reaching approximately 26% analytically and ~15% numerically at 850 RPM and maintaining 13% analytically and 14.25% numerically at 1100 RPM. In contrast, T/C 0.12 drops sharply to 6.46% at 1500 rpm, indicating greater hydrodynamic losses and instability. While all configurations experience declining efficiency as RPM increases, T / C 0.13 consistently maintains better performance, confirming that a higher thickness-to-chord ratio improves hydrodynamic stability and turbine efficiency. The close match between the numerical and analytical results supports the reliability of these findings. However, the validity of the numerical calculations in this study needs to be supported by adequate, apples-to-apples experimental results, which have not yet been provided in the current report. Moreover, an experimental study of the T/C effect on the hydrodynamic performance of propeller turbines is highly recommended for future research.

REFERENCES

[1] National Energy Council, *Indonesia Energy Outlook 2024*. Jakarta: National Energy Council, 2024.

[2] R. Sipayung, "Peningkatan polusi udara di Indonesia: Perspektif ekonomi berdasarkan teori freakonomics," *Sekretariat Kabinet Republik Indonesia*, 2023.

[3] M. Bakırcı, R. Polat, and M. T. Özdemir, "Aerodynamic analysis of NACA 4412 airfoil with CFD for small scale wind turbine design," *J. Green Technol. Environ.*, vol. 1, no. 2, pp. 28–40, 2023.

[4] Ember Energy, "G20 Per Capita Coal Power Emissions 2023." Available: https://ember-energy.org/latest-insights/g20-per-capita-coal-power-emissions-2023/.

[5] Humas EBTKE, "RUPTL 2021-2030 Diterbitkan, Porsi EBT Diperbesar," Direktorat Jenderal Energi Baru, Terbarukan dan Konservasi Energi, Kementerian Energi dan Sumber Daya Mineral. Accessed: Dec. 11, 2023. [Online]. Available: https://ebtke.esdm.go.id/post/2021/10/06/2981/ruptl.2021-2030.diterbitkan.porsi.ebt.diperbesar

[6] D. Zhou and Z. D. Deng, "Ultra-low-head hydroelectric technology: A review," *Renew. Sustain. Energy Rev.*, vol. 78, pp. 23–30, 2017.

[7] R. Risnandar, F. A. Pratama, and N. Novrinaldi, "GIS untuk menentukan potensi pembangunan piko-hidro," *Jurnal Teknologi Informasi*, vol. 1, no. 2, pp. 60–65, 2011.

[8] Y. Wang, C. Jiang, and D. Liang, "Investigation of air-core vortex at hydraulic intakes," *J. Hydrodynamics*, vol. 22, no. 1, pp. 673–678, 2010.

[9] Warjito, Budiarso, K. Kameswara, S. B. S. Nasution, and M. F. Syahputra, "Effect of camber line variations on open flume turbine performance," in *AIP Conference Proceedings*, AIP Publishing LLC, pp. 40008, 2021.

[10] N. Sinaga, B. Yunianto, and Y. V. Pirie, "Effect of thickness-to-chord ratio and chord length on aerodynamics of GOE-387 airfoil," *Int. Res. J. Ind. Eng. Technol.*, vol. 08, no. 05, pp. 280–287, 2024, doi: 10.47001/irjiet/2024.805038.

[11] Z. Markov, P. Popovski, A. Lipej, and V. Djelic, "On the influence of the Kaplan turbine runner blade thickness on its stress parameters," in *International Conference HYDRO*, 2008. p. 111–114.

[12] A. Semenova, D. Chirkov, A. Lyutov, S. Chemy, V. Skorospelov, and I. Pylev, "Multi-objective shape optimization of runner blade for Kaplan turbine," in *IOP Conference Series: Earth and Environmental Science*, pp. 12025, 2014.

[13] M. Banaszek and K. Tesch, "Rotor blade geometry optimization in Kaplan turbine," *TASK Quarterly, Scientific Bulletin of Academic Computer center in Gdansk*, vol. 14, no. 3, pp. 209–225, 2010.

[14] P. Chaitanya and G. S. Sharma, "Computational fluid dynamic analysis of Naca 0006 airfoil at different parameters with regression analysis," *Int. Res. J. Eng. Technol.*, pp. 1027–1034, 2022, [Online]. Available: www.irjet.net

[15] P. Breeze, *"Hydropower." Academic* Press, 2018.
[16] M. Çolak and İ. Kaya, "Prioritization of renewable energy alternatives by using an integrated fuzzy MCDM model: A real case application for Turkey," *Renewable and Sustainable Energy Reviews*, vol. 80, pp. 840–853, 2017, doi: https://doi.org/10.1016/j.rser.2017.05.194.
[17] B. R. Munson, T. H. Okiishi, W. W. Huebsch, and A. P. Rothmayer, *Fluid mechanics*. Singapore: Wiley, 2013.
[18] K. M. Almohammadi, D. B. Ingham, L. Ma, and M. T. T.-C. fluid dynamics (CFD) mesh independency techniques for a straight blade vertical axis wind turbine Pourkashan, "Computational fluid dynamics (CFD) mesh independency techniques for a straight blade vertical axis wind turbine," *Energy*, no. C, pp. 58–483, 2013, doi: 10.1016/j.energy.2013.06.012.
[19] M. Kaya, A. Kök, and H. Kurt, "Comparison of aerodynamic performances of various airfoils from different airfoil families using CFD," *Wind Struct. An Int. J.*, vol. 32, pp. 239–248, Mar. 2021, doi: 10.12989/was.2021.32.3.239.